

WEARABLE IMPEDANCE SENSOR FOR WIRELESS MEASUREMENTS OF PROTEIN BIOMARKERS IN DERMAL INTERSTITIAL FLUID

Elizabeth C. Wilkerson¹, Yan Gong^{2,3}, Wen Li^{2,3}, and Peter B. Lillehoj^{1,4*}

¹Department of Mechanical Engineering, Rice University, Houston, TX, USA

²Department of Electrical and Computer Engineering, Michigan State University, East Lansing, MI, USA

³Institute for Quantitative Health Science & Engineering, Michigan State University, East Lansing, MI, USA and

⁴Department of Bioengineering, Rice University, Houston, TX, USA

ABSTRACT

This paper presents a wearable skin patch for wireless measurements of protein biomarkers in dermal interstitial fluid (ISF). ISF is extracted from the skin using a microneedle (MN)-based, vacuum-assisted technique and autonomously transported through the patch via vacuum pressure. This device was used for quantitative measurements of C-X-C motif chemokine ligand 9 (CXCL9), a biomarker for autoimmune diseases and inflammation, which could be detected from 10 pg/mL to 1,000 pg/mL in phosphate-buffered saline (PBS) with a lower limit of detection of 1.33 pg/mL. Proof-of-concept was demonstrated by performing measurements on cadaver porcine skin dermally injected with ISF simulant spiked with CXCL9, which could be detected at 100 and 1,000 pg/mL, thus validating the functionality of this wearable sensor.

KEYWORDS

Wearable, impedance sensor, wireless, interstitial fluid, diagnostics

INTRODUCTION

Wearable biosensors hold great promise for point-of-care testing and health monitoring due to their automated operation. Prior works have demonstrated wearable sensors capable of rapid and high sensitivity measurements of analytes in bodily fluids, including tattoo-based epidermal sensors for measuring electrolytes in sweat, contact lens sensing platforms for glucose monitoring in tears, and mouthguards with biosensing elements for uric acid analysis in saliva [1]. While these platforms are useful, the detection of protein biomarkers in these fluids offers limited diagnostic utility since they contain only subsets of the biomarkers found in blood and typically at significantly lower concentrations [2].

Prior reports have demonstrated wearable biosensors for the detection of metabolites and circulating drugs in dermal ISF [3], [4], which is a fluid present in the lower viable epidermis and the upper dermis of the skin that has similar biomolecular content as blood [5]–[9]. However, these sensors require bulky components, such as detectors, readers, or batteries, making them uncomfortable and expensive. Wearable sensors with wireless sensing capabilities have been demonstrated for the detection of analytes such as glucose, lactate, uric acid, and tyrosine, in various biofluids [10], [11]. In this work, we have developed a wearable biosensor prototype for wireless measurements of protein biomarkers in dermal ISF. This

device integrates a microfabricated wireless impedance sensor and a microfluidic network into a skin patch. This device is capable of high-sensitivity protein measurements while being compact, lightweight, and disposable.

METHODS

Design and Fabrication of the Impedance Sensor

The impedance sensor consists of a 10 mm-diameter coil antenna (inductor) connected to an interdigitated electrode (IDE) capacitor. Each finger of the IDE is 170 μm wide with an 80 μm separation between the fingers (Fig. 1A). The reader coil is coupled magnetically with the planar coil part of the sensor elements, and a vector network analyzer (VNA) measures the resonance frequency of the entire circuit via the reader antenna. For sensor characterization, a rectangle well was formed around the IDE capacitor using adhesive-backed plastic film to contain the liquid sample during the measurement.

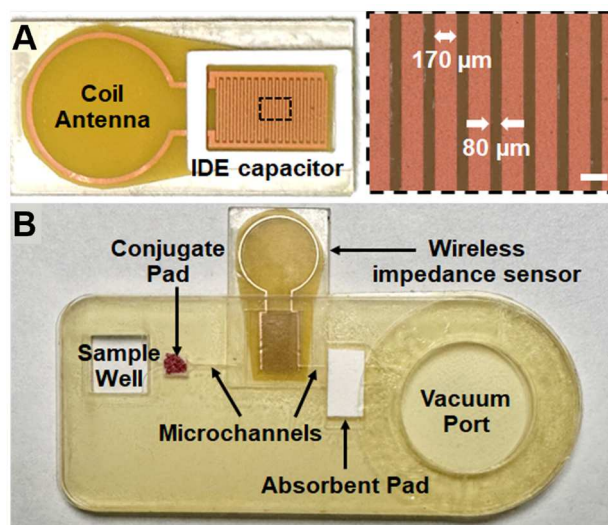


Figure 1: (A) Photograph of the wireless impedance sensor. Inset shows an enlarged view of the IDEs. Scale bar, 200 μm . (B) Photograph of the skin patch prototype with labeled components.

The sensor was fabricated by lithographically patterning thin film copper on a polyimide substrate (Fig. 2). Briefly, a commercial copper-on-polyimide film (DuPont™ Pyralux® AC352500RHV) was cleaned and affixed onto a 4-inch-diameter silicon wafer. The polyimide substrate is 25 μm thick and the copper layer is 35 μm thick. Subsequently, a layer of photoresist (MICROPOSIT™ S1800™ G2 Series Photoresist) was

spin-coated on the film at 3,000 rpm and patterned with ultra-violet (UV) photolithography to form a mask. With this photoresist mask, copper was chemically etched using a 4:1 diluted copper etchant (Ferric Chloride, MG Chemicals). Afterwards, the photoresist was removed from the film using acetone, followed by rinsing with isopropanol alcohol and deionized (DI) water. The sensor was then coated with 40 μm of SU-8 photoresist (Kayaku Advanced Materials) via spin-coating and cured under a 50 W UV light for 2 minutes. Next, the sensor was plasma-treated at 100 W for 15 minutes to facilitate the immobilization of the capture antibody [7]. 30 μL of 1 $\mu\text{g}/\text{mL}$ anti-CXCL9 antibody (Bio-Techne) was dispensed on the IDE region and incubated for 1 hour, washed off with PBS, and dried gently with N_2 . 50 μL of StabilBlock stabilizer solution (SurModics) was incubated on the IDE region for 1 hour and excess solution was removed using a pipette. Sensors were stored with desiccant at 4 $^\circ\text{C}$ and dried overnight.

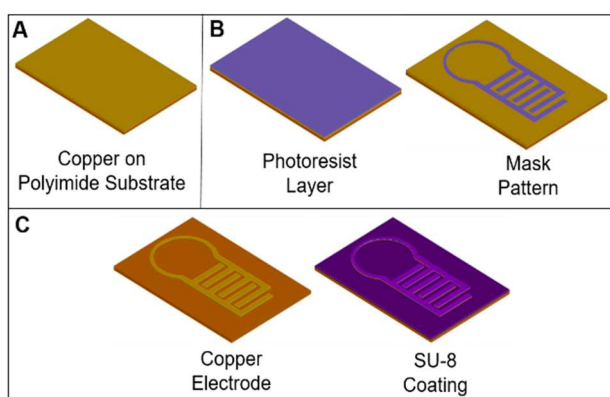


Figure 2: Fabrication process for the wireless impedance sensor consisting of (A) substrate cleaning, (B) photolithographic patterning of photoresist, and (C) copper etching and SU-8 coating.

Design and Fabrication of the Skin Patch

The skin patch consists of an 8 mm \times 8 mm sample well for ISF collection, a 3 mm \times 3 mm cutout for a conjugate release pad which contains gold nanoparticle (AuNP)-antibody conjugates, the impedance sensor, an absorbent pad, and a vacuum port, all of which are connected via a 300 μm -wide, 500 μm -tall microchannel (Fig. 1B). The patch consists of 1 layer of 3 mm-thick polymethylmethacrylate (PMMA) (McMaster Carr), 1 layer of 105 μm -thick polyethylene terephthalate (PET) (Optiazure) and 2 layers of double-sided adhesive tape (3M Company and Adhesives Research, Inc.) which contain cutouts and microfluidic elements. The layers were designed in AutoCAD software and fabricated using a CO_2 laser cutter (Universal Laser Systems). The patch was assembled by adhering the PMMA and PET layers together using the double-sided adhesive tape and the impedance sensor was integrated within the layers.

Preparation of AuNP-Antibody Conjugates and the Conjugate Release Pad

AuNP-antibody conjugates were prepared by incubating 80 μL of 30 nm OD-1 AuNPs (Sigma Aldrich) with 5 μL of biotinylated anti-CXCL9 antibody (Bio-

Techne) for 1 hour with gentle shaking. Bovine serum albumin (BSA) (Sigma-Aldrich) was then added to the AuNP-antibody conjugate solution and incubated for 1 hour with gentle shaking. The solution was centrifuged at 9,000 rpm for 10 minutes, the supernatant was removed, and the pellet was resuspended in a solution containing 20% sucrose (Sigma-Aldrich) in Stabilblock immunostabilizer (SurModics) and 5% Tween-20 (Sigma-Aldrich) in DI water. The AuNP-antibody conjugate solution was stored at 4 $^\circ\text{C}$.

Conjugate release pads were created from glass fiber strips (Millipore Sigma) soaked in a PBS solution containing 10% sucrose, 2% BSA, and 0.25% Tween-20 for 2 hours at 4 $^\circ\text{C}$. The strips were then dried at 38 $^\circ\text{C}$ for 2 hours and cut into \sim 3 mm \times 3 mm pads. 3 μL of AuNP-antibody conjugate solution was dispensed on the conjugate pads and dried for 1 hour at 38 $^\circ\text{C}$.

Fabrication of the MN Array

MN arrays were designed in NX software and 3D printed using a Photonic Professional GT lithography system (Nanoscribe). MN arrays were fabricated via centrifugation-assisted replica molding in polydimethylsiloxane (PDMS) (Sylgard 184). SU-8 2025 photoresist (Kayaku Advanced Materials) was poured into the PDMS molds, centrifuged at \sim 3,500 rpm for 15 minutes, and cured under a 50W UV lamp for 3 minutes. MN array replicas were removed from the mold and coated with 1.5 μm of parylene C using a Labcoater 2 parylene deposition system (Specialty Coating Systems).

Wireless Measurements Using the Skin Patch

Micropores were first generated in the skin via insertion of the MN array using a spring-loaded applicator (Micropoint Technologies). The patch was attached to the skin and positioned so that the opening for the sample was aligned over the MN insertion site. A 30-mm diameter suction cup (Hansol Medical) was attached to the vacuum port of the patch and vacuum pressure was generated for 1 hour using a hand pump (Hansol Medical). The vacuum pressure caused ISF to be extracted from the micropores where it was subsequently transported to the conjugate pad,

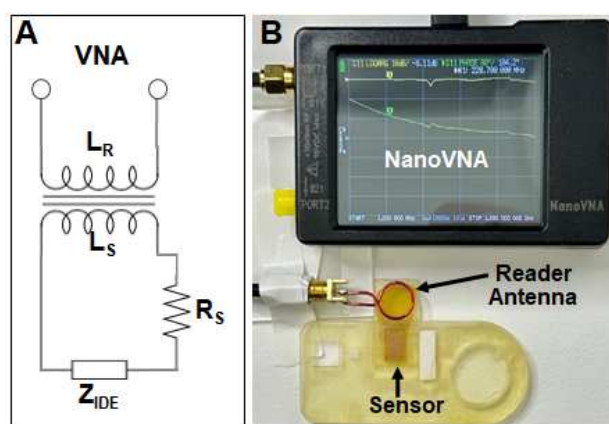


Figure 3: (A) Equivalent circuit for the sensor. L_R = reading coil inductance, L_S = sensor inductance, R_S = sensor resistance, and Z_{IDE} = IDE impedance. (B) Photograph depicting the experimental set-up for wireless measurements.

reconstituting the AuNP-antibody conjugates. In the presence of CXCL9, CXCL9-AuNP-antibody complexes were formed, which subsequently bound to the capture antibody-immobilized IDE region. This altered the conductivity of the liquid sample, thereby changing the impedance and resonance frequency of the sensor, as depicted in the equivalent resonant circuit of the sensor (Fig. 3A). In the absence of CXCL9, the AuNP-antibody conjugates were washed away, resulting in a negligible change in the sensor impedance. The frequency response of the sensor was measured wirelessly via the inductor coil using a NanoVNA (Fig. 3B).

RESULTS AND DISCUSSION

Fluid Extraction Capability of the Skin Patch

The ability for ISF to be extracted from skin and transported through the patch via suction was evaluated using an artificial skin model consisting of blue dye solution in 2% agar covered in Parafilm. As shown in Fig. 4, the solution was quickly extracted from the micropores, and the AuNP-antibody conjugates were reconstituted as the liquid flowed through the conjugate pad. The solution filled the IDE sensing region within 2 minutes.

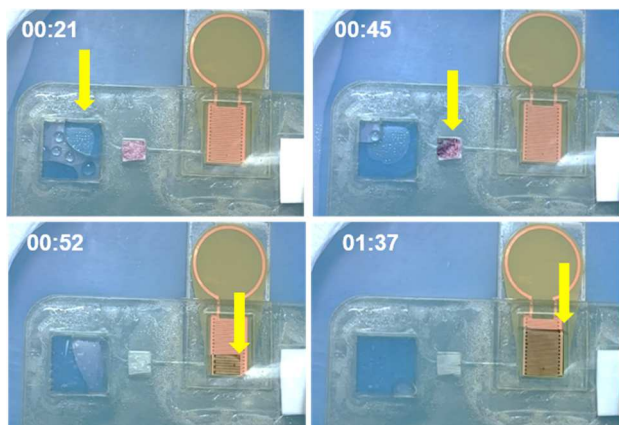


Figure 4: Still frame images showing the extraction and transport of colored dye through the microfluidic network. Time stamps (min:sec) are located in the upper left corners. Arrows indicate the position of the liquid front.

The design of the microfluidic network, including the channels and chamber over the IDE sensing region, were optimized to ensure that the extracted fluid could be transported through the device and remain in the IDE sensing region for the duration of the incubation period. Additionally, the dimensions of the microfluidic network were optimized to minimize the volume of fluid required for each measurement (30 μ L), which could be extracted from the skin model within 2 minutes.

Wireless Measurements of CXCL9 in PBS

The impedance sensor was characterized using PBS samples spiked with varying concentrations of CXCL9. CXCL9 is a biomarker for autoimmune diseases and inflammation and is present in various biofluids, including ISF, at concentrations ranging from 100 – 1,000 pg/mL [12], [13]. For this study, measurements were performed

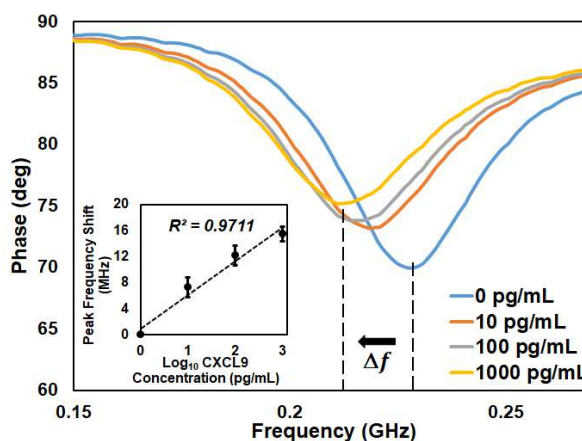


Figure 5: Phase vs. frequency curves for varying concentrations of CXCL9 spiked in PBS samples. Inset shows the corresponding peak frequency shift (Δf) vs. CXCL9 concentration. Each data point represents the mean \pm standard deviation of three trials.

using PBS due to its similarity in ion concentration, osmolarity, and pH as human bodily fluids [8]. As shown in Fig. 5, distinct phase vs. frequency curves were generated for different CXCL9 concentrations. The change in frequency between the peak frequency of each concentration was recorded and a linear response was observed ($R^2=0.9711$). The lower limit of detection of this sensor was calculated to be 1.33 pg/mL [14].

Proof-of-Concept Demonstration

Proof-of-concept demonstration of the skin patch was carried out by performing measurements on cadaver porcine skin dermally injected with 30 μ L of ISF simulant (1.3 mg/mL bovine serum albumin in Tyrode's salts) [15] spiked with varying concentrations of CXCL9 (0, 100 and 1,000 pg/mL). The peak frequency shift at different CXCL9 concentrations was calculated from the phase vs. frequency values, which resulted in a linear response in the

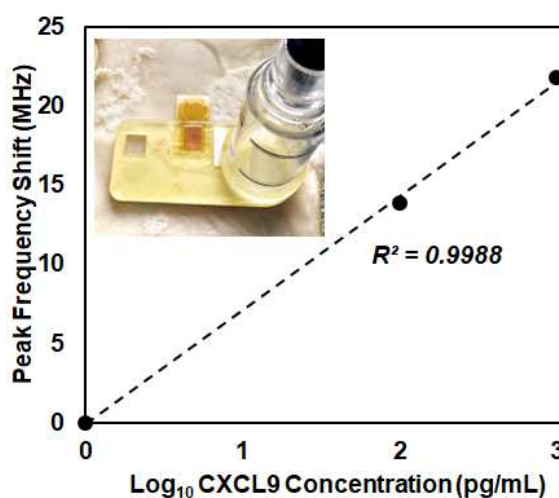


Figure 6: Peak frequency shift vs. CXCL9 concentration measured on cadaver porcine skin dermally injected with ISF simulant spiked with CXCL9. Inset shows the skin patch prototype (with the vacuum cup attached) on porcine skin during the measurement.

peak frequency shift ($R^2=0.9988$). The increase in peak frequency shift with higher CXCL9 concentrations validated the functionality of this device for *in vivo* protein measurements (Fig. 6).

CONCLUSIONS

We have developed a skin patch prototype for wireless measurements of protein biomarkers in dermal ISF. The sensor was characterized by performing measurements of PBS samples spiked with CXCL9, which could be detected at concentrations from 10 to 1,000 pg/mL with excellent linearity and a lower limit of detection of 1.33 pg/mL. CXCL9 could be detected in cadaver porcine skin dermally injected with spiked ISF simulant, validating the functionality of this device for *in vivo* protein measurements. The ability to wirelessly detect protein biomarkers in dermal ISF with high sensitivity in a user-friendly manner is a promising approach for various clinical applications including point-of-care testing and health monitoring.

ACKNOWLEDGEMENTS

We acknowledge the Shared Equipment Authority of Rice University for the use of the cleanroom facilities to fabricate the MN arrays. This research was funded in part by the Wellcome Trust [215826/Z/19/Z]. Wilkerson provided work supported by the National Science Foundation Graduate Research Fellowship [1842494]. Travel support was provided in part by the Liu Idea Lab for Innovation and Entrepreneurship at Rice University.

REFERENCES

- [1] J. Kim, A. S. Campbell, B. E. F. de Ávila, and J. Wang, "Wearable biosensors for healthcare monitoring," *Nat. Biotechnol.*, vol. 37, no. 4, pp. 389–406, 2019, doi: 10.1038/s41587-019-0045-y.
- [2] D. Sim *et al.*, "Biomarkers and Detection Platforms for Human Health and Performance Monitoring: A Review," *Adv. Sci.*, vol. 9, no. 7, pp. 1–29, 2022, doi: 10.1002/advs.202104426.
- [3] M. Friedel *et al.*, "Opportunities and challenges in the diagnostic utility of dermal interstitial fluid," *Nat. Biomed. Eng.*, 2023, doi: 10.1038/s41551-022-00998-9.
- [4] S. Lin *et al.*, "Wearable microneedle-based electrochemical aptamer biosensing for precision dosing of drugs with narrow therapeutic windows," *Sci. Adv.*, vol. 8, no. 38, pp. 1–14, 2022, doi: 10.1126/sciadv.abq4539.
- [5] P. P. Samant and M. R. Prausnitz, "Mechanisms of sampling interstitial fluid from skin using a microneedle patch," *Proc. Natl. Acad. Sci. U. S. A.*, vol. 115, no. 18, pp. 4583–4588, 2018, doi: 10.1073/pnas.1716772115.
- [6] B. Q. Tran *et al.*, "Proteomic Characterization of Dermal Interstitial Fluid Extracted Using a Novel Microneedle-Assisted Technique," *J. Proteome Res.*, vol. 17, no. 1, pp. 479–485, 2018, doi: 10.1021/acs.jproteome.7b00642.
- [7] A. C. Müller *et al.*, "A comparative proteomic study of human skin suction blister fluid from

healthy individuals using immunodepletion and iTRAQ labeling," *J. Proteome Res.*, vol. 11, no. 7, pp. 3715–3727, 2012, doi: 10.1021/pr3002035.

- [8] F. Ribet *et al.*, "Microneedle Patch for Painless Intradermal Collection of Interstitial Fluid Enabling Multianalyte Measurement of Small Molecules, SARS-CoV-2 Antibodies, and Protein Profiling," *Adv. Healthc. Mater.*, vol. 2202564, pp. 1–11, 2023, doi: 10.1002/adhm.202202564.
- [9] P. R. Miller *et al.*, "Extraction and biomolecular analysis of dermal interstitial fluid collected with hollow microneedles," *Commun. Biol.*, vol. 1, no. 1, 2018, doi: 10.1038/s42003-018-0170-z.
- [10] G. Ertürk and B. Mattiasson, "Capacitive biosensors and molecularly imprinted electrodes," *Sensors (Switzerland)*, vol. 17, no. 2, pp. 1–21, 2017, doi: 10.3390/s17020390.
- [11] B. Senf, W. H. Yeo, and J. H. Kim, "Recent Advances in Portable Biosensors for Biomarker Detection in Body Fluids," *Biosensors*, vol. 10, no. 9, 2020, doi: 10.3390/BIOS10090127.
- [12] C. Y. Ng *et al.*, "Skin Interstitial Fluid and Plasma Multiplex Cytokine Analysis Reveals IFN- γ Signatures and Granzyme B as Useful Biomarker for Activity, Severity and Prognosis Assessment in Vitiligo," *Front. Immunol.*, vol. 13, no. April, pp. 1–10, 2022, doi: 10.3389/fimmu.2022.872458.
- [13] K. Szegedi *et al.*, "Cytokine profiles in interstitial fluid from chronic atopic dermatitis skin," *J. Eur. Acad. Dermatology Venereol.*, vol. 29, no. 11, pp. 2136–2144, 2015, doi: 10.1111/jdv.13160.
- [14] J. Li and P. B. Lillehoj, "Microfluidic Magneto Immunosensor for Rapid, High Sensitivity Measurements of SARS-CoV-2 Nucleocapsid Protein in Serum," *ACS Sensors*, vol. 6, no. 3, pp. 1270–1278, 2021, doi: 10.1021/acssensors.0c02561.
- [15] X. Jiang *et al.*, "Microneedle-based skin patch for blood-free rapid diagnostic testing," *Microsystems Nanoeng.*, vol. 6, no. 1, pp. 1–11, 2020, doi: 10.1038/s41378-020-00206-1.

CONTACT

*Peter B. Lillehoj, lillehoj@rice.edu